Promoting the flash sintering of ZnO in reduced atmospheres to achieve nearly full densities at furnace temperatures of <120 °C

Yuanyao Zhang and Jian Luo[*]

Department of NanoEngineering, Program of Materials Science and Engineering, University of California, San Diego, La Jolla, CA 92093, USA

Using ZnO as a model system, a strong dependence of the onset flash sintering temperature on the atmosphere has been discovered. In the best cases, ZnO specimens have been sintered to >97% relative densities (with fine grain sizes of ~1 μm) in ~30 s at furnace temperatures of <120 °C in Ar + 5 mol.% H_2. The enhanced conductivities of ZnO powder specimens in reduced atmospheres are responsible for the substantial decreases of the onset flash sintering temperatures.

Recently, Raj and co-workers invented "flash sintering," which has attracted significant scientific and technological interests because it can achieve high densities in short durations at much reduced furnace temperatures [1,2]. Flash sintering of a broad range of oxide-based ion/mixing conductors (e.g., Y_2O_3-stablized ZrO_2 [2,3], $La_{0.6}Sr_{0.4}Co_{0.2}Fe_{0.8}O_3$ [4], $Ce_{0.8}Gd_{0.2}O_{1.9}$ [5]) and semiconductors (e.g., Co_2MnO_4 [6,7], TiO_2 [8], ZnO [9,10], Y_2O_3 [11], and $SrTiO_3$ [12]), as well as several non-oxide ceramics (e.g. SiC [13] and ZrB_2 [14]), has been demonstrated.

Specifically, flash sintering at ultra-low furnace temperatures can have significant technological advantages, e.g., as an energy-saving fabrication method for consolidating ceramics. In an effort to greatly reduce the flash sintering temperature, Down and Sglavo applied a high electric field of 2250 V/cm to 8 mol.% Y_2O_3-stablized ZrO_2 (8YSZ); they showed that the onset flash sintering temperature could be decreased to 390 °C, but the specimen could not be sintered to a high density (having achieved only 8.5% linear shrinkage in comparison to achieving a maximum of 28.1% linear shrinkage with a lower applied field/higher onset flash sintering temperature) [15]. While both AC and DC flash sintering ZnO in air has been conducted recently [9,10], this study demonstrated, for the first time to our knowledge, a strong dependence of the onset flash sintering temperature on the atmosphere (air vs. O_2, Ar and Ar-H_2) using ZnO as a model system, suggesting a new method to control and induce flash sintering. Pursing along this line, we found a set of conditions to flash-sinter ZnO specimens to >97% of the theoretical density in ~30 s at furnace temperatures of <120 °C in a reduced hydrogen atmosphere (Ar + 5 mol.% H_2).

High-purity ZnO powders (>99.99%, purchased from Sigma Aldrich; the particle size provided by the vendor is 30 nm; noting that the measured grain size is ~100 nm for the green specimens after burning the binder at 500 °C for one hour, before the flash sintering experiments) were ground in Al_2O_3 media for 0.5 h with 0.5 wt.% of a binder (3 wt.% of PVA dissolved in water). The granulated powders were uniaxially pressed at ~300 MPa to make green specimens with the approximate dimensions: D (diameter) = 6.4 mm and H (height) = 1 mm. The average bulk densities of the green specimens were measured to be 62.0% (with a standard deviation of 1.0%). The green specimens were baked at 500 °C for one hour to burn out the binders (with no significant shrinkages). Platinum was sputtered on the both sides of the green specimens using a Denton Discovery 18 Sputtering System. The sides of the sputtered specimens were slightly grounded by SiC papers after sputtering. Specimens were then placed in a horizontal tube furnace and attached with Pt wires on both sides to apply an electric field. These flash sintering experiments were conducted either in air or in a flow of gas (Ar, Ar + 5 mol.% H_2 and O_2, respectively); in the latter case, the furnace tube was purged by the specific gas for half an hour before heating; then, a constant gas flow maintained in the tube furnace during the entire course of experiments. Similar to a typical flash sintering experiment, the applied voltage was kept constant until the resultant current reach a preset maximum value (I_{max} = 1 and 4 A,

[*] Corresponding author; e-mail: jluo@alum.mit.edu

respectively; corresponding to estimated maximum current densities: $J_{max} \approx 39$ or 153 mA/mm^2, respectively), at which point the power source was switched from voltage to current control. The electric power source and furnace were shut down after 30 s when the power density reached the maximum, and the specimens were cooled down within the furnace. Final bulk densities were measured by the standard Archimedes method. The microstructure was determined by the field emission environmental scanning electron microscope (SEM, Philips XL30). Grain sizes were measured at the fracture surfaces using a standard intercept method from SEM micrographs.

Figure 1(a) shows the electric power density *vs.* the furnace temperature (T_F) curves for the ZnO samples sintered under an (initial) applied electric field of $E = 300 \text{ V/cm}$, with I_{max} being set to 1 A ($J_{max} \approx 39 \text{ mA/mm}^2$). AC and DC flash sintering ZnO in air has been conducted before [9,10]; in this study, we further conducted flash sintering experiments of ZnO in three different flowing gases (Ar, Ar + 5 mol.% H₂, and O₂, respectively) to compare the results with those obtained in air under identical E and I_{max} conditions (Fig. 1(a)).

The most significant discovery of this study is that the onset flash temperature for the ZnO specimen depends strongly on the sintering atmosphere (Fig. 1(a) and Table 1). Specifically, sintering in an inert (reducing) Ar atmosphere decreased the onset of flash sintering temperature (from 599 °C in air) to 237 °C. Sintering in a more reducing hydrogen atmosphere (Ar + 5 mol.% H₂) further
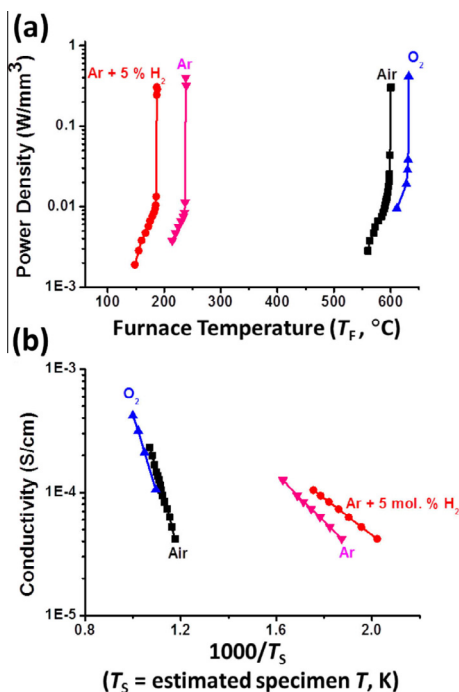

Figure 1. (a) Measured electric power dissipation *vs.* furnace temperature curves for the flash sintering of ZnO in four different atmospheres, where the applied electric field was set to be 300 V/cm. (b) Measured conductivity *vs.* the reciprocal of the estimated specimen temperature curves. The measured conductivities shown in panel (b) can be used to predict the observed onset flash sintering temperatures shown in panel (a) for all four cases using the model proposed in Ref. [10] and discussed in Supplementary material, as shown in Supplementary Fig. S1.

lowered the onset of flash sintering temperature to 186 °C. Consistently, sintering in pure O₂ increased the onset flash sintering temperature slightly (from 599 °C in air) to 631 °C.

The dependence of the onset flash sintering temperature on the atmosphere can be explained from the increased conductivities of ZnO in reducing atmospheres. To illustrate this, we plotted the conductivity (in a logarithmical scale) *vs.* the reciprocal of (absolute) specimen temperature curves in Figure 1(b) for the virtually identical ZnO powder specimens measured in four different atmospheres (before the occurrence of a flash event); here, the specimen temperatures (T_S) were estimated from a black-body radiation model proposed by Raj [16], which are also listed in Table 1. In all cases, the temperature-dependent conductivities follow an Arrhenius relation (see Supplementary material for a detailed analysis of Arrhenius fitting). Figure 1(b) (as well as Table SI in the Supplementary material) shows that the activation energy is lower for specimens measured in reduced atmospheres (Ar and Ar + 5 mol.% H₂). Consequently, the conductivity can be increased substantially to trigger flash events at much lower temperatures in reduced atmospheres (Ar and Ar + 5 mol.% H₂).

In fact, it is well documented that the electric conductivity of (dense) polycrystalline ZnO specimens would increase with decreasing oxygen partial pressures [17]. Increases of the conductivities of ZnO in H₂ have also been reported [18,19]. First-principle calculations [20–22] further suggested that the hydrogen interstitials could be shallow donors; thus, the incorporation of hydrogen into ZnO may further increase the conductivity by doping in addition to the simple reduction effects to further lower the onset flash sintering temperature.

Two recent independent studies suggested that flash sintering of ZnO [10] and 3YSZ [23] starts as a thermal runaway and the onset flash sintering temperature is essentially identical to the thermal runaway temperature predicted from the measured conductivity *vs.* temperature function (noting that this thermal runaway model only explains how the flash sintering starts but not how densification occurs). A brief introduction of this thermal runaway model (for predicting onset flash sintering temperature), along with the analysis of the current four sets of data (obtained in four different atmospheres), is given in the Supplementary material. This model, using the measured conductivity *vs.* temperature functions, can predict the thermal runaway temperatures that are consistent with the observed onset flash sintering (furnace) temperatures for experiments conducted in all four atmospheres with high accuracies, as shown in the Supplementary Fig. S1 and summarized in Table 1. Thus, this thermal runaway model (discussed in the Supplementary material) quantitatively demonstrates that the decreases in the onset flash sintering temperatures in Ar and Ar + 5 mol.% H₂ are results of the increased conductivities at lower temperatures (Fig. 1(b)) in reduced atmospheres (Fig. 1(b)) [17–19] while the incorporation of hydrogen interstitials as shallow donors [20–22] may help further.

While the initial densities of all green specimens were around 62%, the final densities after the flash sintering are 64.0%, 69.0%, 97.5% and 94.8%, for specimens flash-sintered in Ar + 5 mol.% H₂, Ar, Air and O₂, respectively, for ~30 s with the experimental conditions of $E = 300 \text{ V/cm}$ and $I_{max} = 1$ A (Table 1). This suggests that although the ZnO specimens have been successfully

Table 1. Summary of the key experimental results of the flash sintering experiments. The onset flash sintering temperature is defined as the furnace temperature when a sharp rise in the power density occurred. The specimen temperatures (T_S) were estimated from the Raj model [14] for the first four cases ($E = 300$ V/cm), and based on the observation of the melting of sputtered Pt electrodes and non-melting of ZnO for the latter four cases (see text for details).

Flash sintering conditions	Atmosphere	Sintered relative density (%)	Before the flash (onset flash)		In the flash state	
			Furnace temperature (T_F, °C)		Estimated specimen temperature (T_S, °C)	
			Experimental	Predicted*		
$E = 300$ V/cm, $I_{max} = 1$ A	Ar + 5 mol.% H$_2$	64.0	186	187	328	783
	Ar	69.0	237	238	341	943
	Air	97.5	599	598	675	1083
	O$_2$	94.8	631	632	727	1169
$E = 500$ V/cm, $I_{max} = 4$ A	Ar + 5 mol.% H$_2$	97.4	108	–	240	>1772; ≪1975
	Ar + 5 mol.% H$_2$	90.1	127	–	275	>1772; ≪1975
$E = 1000$ V/cm, $I_{max} = 4$ A	Ar + 5 mol.% H$_2$	97.7	116	–	–	>1772; ≪1975
	Ar + 5 mol.% H$_2$	93.0	120	–	–	>1772; ≪1975

* The furnace temperatures (T_F) for the onset of the flash event were predicted from the thermal runaway model for the first four cases (see Supplementary materials and Supplementary Fig. S1 for details), which agree well with experimental observations.

sintered to high densities in Air and O$_2$, the densification was limited for specimens sintered in Ar and Ar + 5 mol.% H$_2$ under this specific set of experimental conditions. The estimated specimen temperatures at the activated states (the steady state after the onset flash) from the Raj model [14] were 1083 °C and 1169 °C, respectively, for specimens flash-sintered in Air and O$_2$, respectively; however, estimated specimen temperatures were only 783 °C and 943 °C, for specimens sintered in Ar + 5 mol.% H$_2$ and Ar, respectively (Table 1). The significantly lower specimen temperatures for the two latter cases explain the low densification in Ar + 5 mol.% H$_2$ and Ar with the specific experimental conditions of $E = 300$ V/cm and $I_{max} = 1$ A (Table 1).

To further reduce the onset flash sintering temperature and simultaneously increase the densification, we conducted four additional flash sintering experiments of ZnO powder specimens in Ar + 5 mol.% H$_2$ at higher applied electrical fields ($E = 500$ V/cm and 1000 V/cm) with a greater maximum current limit ($I_{max} = 4$ A or $J_{max} \approx 153$ mA/mm^2). Two specimens were prepared for each condition.

Figure 2 shows the electric powder density *vs.* furnace temperature curves for the flash sintering of ZnO powder specimens in Ar + 5 mol.% H$_2$ with the experimental conditions of $E = 500$ or 1000 V/cm and $I_{max} = 4$ A; the relevant
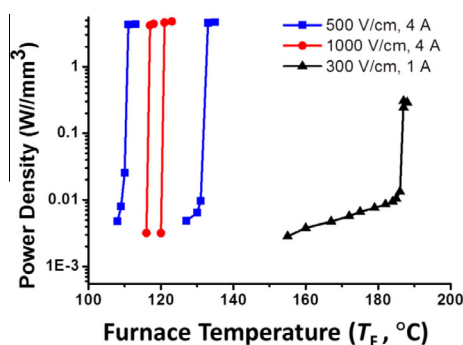
results are also summarized in Table 1. Specifically, the onset of flash temperatures was measured in the range of 110–130 °C (with ∼20 °C specimen-to-specimen variations) with the higher applied electric fields. While the estimated specimen temperatures from the Raj model [14] were ∼2000 °C, such estimation might be inaccurate because Pt melts at 1772 °C; consequently, the contact resistance changed due to the melting (and dewetting) of sputtered Pt electrodes (see Supplementary Fig. S2) so that a simple model is no longer accurate. On the one hand, we observed the (partial) melting of the sputtered Pt electrodes (while the contacting Pt wires still remained intact/did not melt); thus, we believe that the specimen temperature should be (slightly) higher than the melting temperature of Pt (1772 °C). On the other hand, the micrographs of flash-sintered ZnO (Fig. 3) show relatively small grains (∼1 μm) without any indication of melting; thus, the actual specimen temperature should appreciably lower the melting temperature of ZnO (1975 °C). The final sintered densities were measured to be in the range of ∼90–98% of the
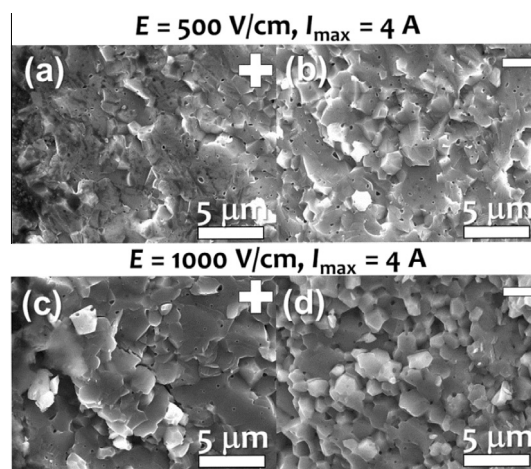

Figure 2. Measured electric power dissipation *vs.* furnace temperature curves for the flash sintering of ZnO in Ar + 5 mol.% H$_2$ with different applied electric fields.

Figure 3. SEM micrographs of the (a, c) anode and (b, d) cathode sides of the fractured surfaces of flash-sintered ZnO specimens, where the initial applied electric field was set to be (a, b) 500 V/cm and (c, d) 1000 V/cm, respectively.

theoretical density. Two best specimens achieved >97% of the theoretical density.

It is interesting to note that the onset flash sintering temperature is almost the same with the applied electric field of 500 V/cm or 1000 V/cm. Presumably, at such lower temperatures, the kinetics for the reduction reaction of ZnO with the hydrogen gas, as well as the possible incorporation of hydrogen interstitials, is limited. Thus, a higher applied electric field will not help further, and the flash will not start until reaching a certain minimum temperature ($\sim$110–130 °C) when ZnO can be partially reduced to have sufficient conductivity. This hypothesis is consistent with experimental observations (Fig. 2). It is worth noting that a somewhat similar effect of a small decrease of onset flash sintering with a large increase of applied electric field was evident in a prior study of 3YSZ for applied electric fields near 1000 V/cm [23], where the underlying mechanism may be different.

Figure 3 shows the microstructures of the fractured surfaces of the flash-sintered specimens (with the experimental conditions: $E = 500$ V/cm and 1000 V/cm; $I_{max} = 4A$; 30 s). The grain sizes were measured to be $1.0 \pm 0.3\,\mu m$ at the anode side and $0.9 \pm 0.3\,\mu m$ at the cathode side, respectively, for the specimens flash-sintered at 500 V/cm. The grain sizes were measured to be $1.4 \pm 0.5\,\mu m$ at the anode side and $1.3 \pm 0.4\,\mu m$ at the cathode side, respectively, for the specimens flash-sintered at 1000 V/cm. It is interesting to note that the grain sizes are virtually identical at the anode and cathode sides in the current cases. This differs from a prior report of the specimens flash-sintered at a lower applied electric field of $E = 300$ V/cm in air, where an abnormal grain growth and/or coarsening at the anode-side was observed [10]. This is presumably due to a reduction effect in Ar + 5 mol.% H_2 that offsets the selected grain boundary oxidation at the anode size in air, as proposed as the underlying mechanism for the anode-side grain boundary (complexion [24]) transition and abnormal grain growth in the prior study [10].

In summary, this study demonstrated the onset flash sintering temperature of ZnO can be significantly decreased in reducing atmospheres. This discovery of significant dependence of flash sintering behaviors on atmosphere suggests a new method to control flash sintering via controlling the sintering atmosphere. A set of experimental conditions have been found, enabling the high-purity ZnO powder specimens to be flashed sintered to >97% of the theoretical density with fine grain sizes of $\sim$1 μm in $\sim$30 s at furnace temperatures of <120 °C in Ar + 5 mol.% H_2. The significant decreases in the onset flash sintering temperatures in reduced atmospheres can be well explained from increased conductivities of ZnO, as quantitatively supported by a thermal runaway model detailed in the Supplementary material.

[1] R. Raj, M. Cologna, J.S.C. Francis, J. Am. Ceram. Soc. 94 (2011) 1941–1965.
[2] M. Cologna, B. Rashkova, R. Raj, J. Am. Ceram. Soc. 93 (2010) 3556–3559.
[3] M. Cologna, A.L.G. Prette, R. Raj, J. Am. Ceram. Soc. 94 (2011) 316–319.
[4] A. Gaur, V.M. Sglavo, J. Mater. Sci. 49 (2014) 6321–6332.
[5] X. Hao, Y. Liu, Z. Wang, J. Qiao, K. Sun, J. Power Sources 210 (2012) 86–91.
[6] A.L.G. Prette, M. Cologna, V. Sglavo, R. Raj, J. Power Sources 196 (2011) 2061–2065.
[7] A. Gaur, V.M. Sglavo, J. Eur. Ceram. Soc. 34 (2014) 2391–2400.
[8] S.K. Jha, R. Raj, J. Am. Ceram. Soc. 97 (2014) 527–534.
[9] C. Schmerbauch, J. Gonzalez-Julian, R. Roeder, C. Ronning, O. Guillon, J. Am. Ceram. Soc. 97 (2014) 1728–1735.
[10] Y. Zhang, J.I. Jung, J. Luo, Acta Mater. 94 (2015) 87–100.
[11] H. Yoshida, Y. Sakka, T. Yamamoto, J.M. Lebrun, R. Raj, J. Eur. Ceram. Soc. 34 (2014) 991–1000.
[12] A. Karakuscu, M. Cologna, D. Yarotski, J. Won, J.S.C. Francis, R. Raj, B.P. Uberuaga, J. Am. Ceram. Soc. 95 (2012) 2531–2536.
[13] E. Zapata-Solvas 1, S. Bonilla, P.R. Wilshaw, R.I. Todd, J. Eur. Ceram. Soc. 33 (2013) 2811–2816.
[14] S. Grasso, T. Saunders, H. Porwal, O. Cedillos-Barraza, D.D. Jayaseelan, W.E. Lee, M.J. Reece, J. Am. Ceram. Soc. 97 (2014) 2405–2408.
[15] J.A. Down, V.M. Sglavo, J. Am. Ceram. Soc. 96 (2013) 1342–1344.
[16] R. Raj, J. Eur. Ceram. Soc. 32 (2012) 2293–2301.
[17] J. Lee, J.H. Hwang, J.J. Mashek, T.O. Mason, A.E. Miller, R.W. Siegel, J. Mater. Res. 10 (1995) 2295–2300.
[18] S.J. Baik, J.H. Jang, C.H. Lee, W.Y. Cho, K.S. Lim, Appl. Phys. Lett. 70 (1997) 3516–3518.
[19] S. Kohiki, M. Nishitani, T. Wada, T. Hirao, Appl. Phys. Lett. 64 (1994) 2876.
[20] C.G. Van de Walle, J. Neugebauer, Nature 423 (2003), 626-528.
[21] C.G. Van de Walle, Phys. Status Solidi B 235 (2003) 89–95.
[22] A. Janotti, C.G. Van de Walle, Nat. Mater. 6 (2007) 44–47.
[23] R.I. Todd, E. Zapata-Solvas, R.S. Bonilla, T. Sneddon, P.R. Wilshaw, J. Eur. Ceram. Soc. 35 (2015) 1865–1877.
[24] P.R. Cantwell, M. Tang, S.J. Dillon, J. Luo, G.S. Rohrer, M.P. Harmer, Acta Mater. 62 (2014) 1–48.